

## SUPPORTING INFORMATION

Anode coverage for enhanced electrochemical oxidation: a green  
and efficient strategy towards water-dispersible graphene

*Huishan Wang,<sup>†, &</sup> Suyun Tian,<sup>†, ‡</sup> Siwei Yang,<sup>†, &</sup> Gang Wang,<sup>‡\*</sup> Xiaofei You,<sup>†, &</sup>  
Lixuan Xu,<sup>†, &</sup> Qingtian Li,<sup>†, &</sup> Peng He,<sup>†, &, \*</sup> Guqiao Ding,<sup>†, &, \*</sup> Zhi Liu<sup>†, &, ‡</sup> and  
Xiaoming Xie<sup>†, &, ‡</sup>*

<sup>†</sup>Center for Excellence in Superconducting Electronics, State Key Laboratory of  
Functional Materials for Informatics, Shanghai Institute of Microsystem and  
Information Technology, Chinese Academy of Sciences, 865 Changning Road,  
Shanghai 200050, P. R. China.

<sup>&</sup>University of Chinese Academy of Sciences, Beijing, 100049, P. R. China.

<sup>‡</sup>School of Physical Science and Technology, ShanghaiTech University, Shanghai  
200031, P. R. China.

<sup>‡\*</sup>Department of Microelectronic Science and Engineering, Faculty of Science,  
Ningbo University, Ningbo 315211, P. R. China.

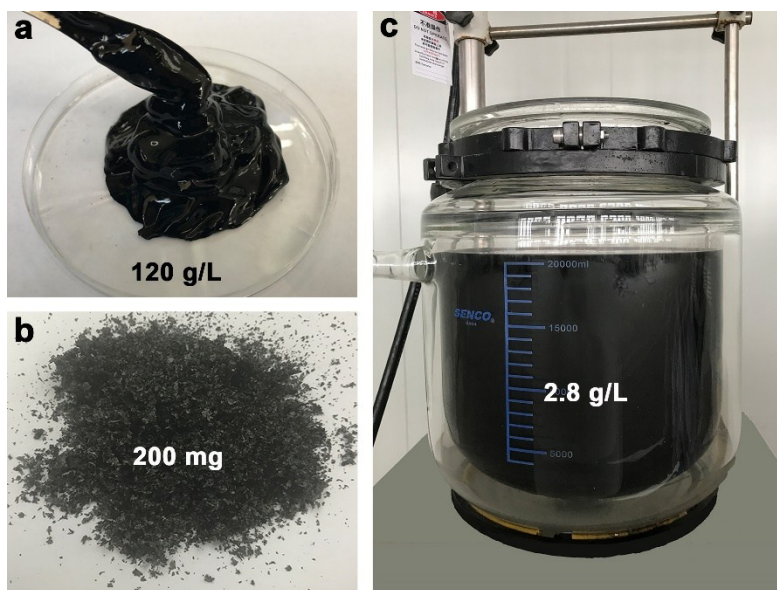


**Fig. S1.** (a) W-Gr aqueous slurry with ultrahigh concentration of 120 g/L. (b) Digital photographs of 200 mg W-Gr powder. (c) 20.0 L W-Gr aqueous solution with a concentration of 2.8 g/L.

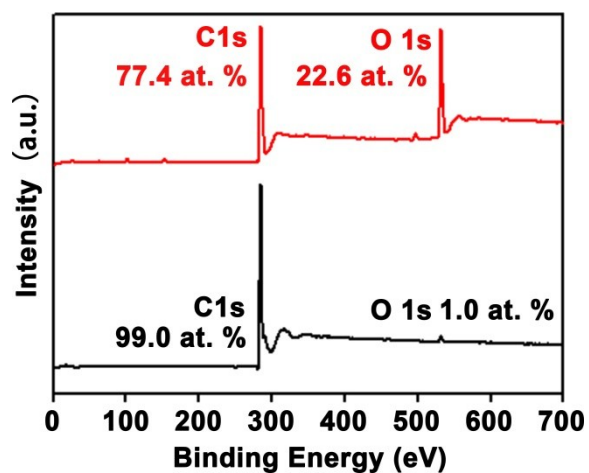


**Fig. S2.** The XPS survey spectra of graphite foil (black line) and obtained W-Gr. The two peaks of W-Gr at 533.0 eV and 285.0 eV are attributed to the O 1s and C 1s peak, respectively, which proved the oxygen functional groups on W-Gr.

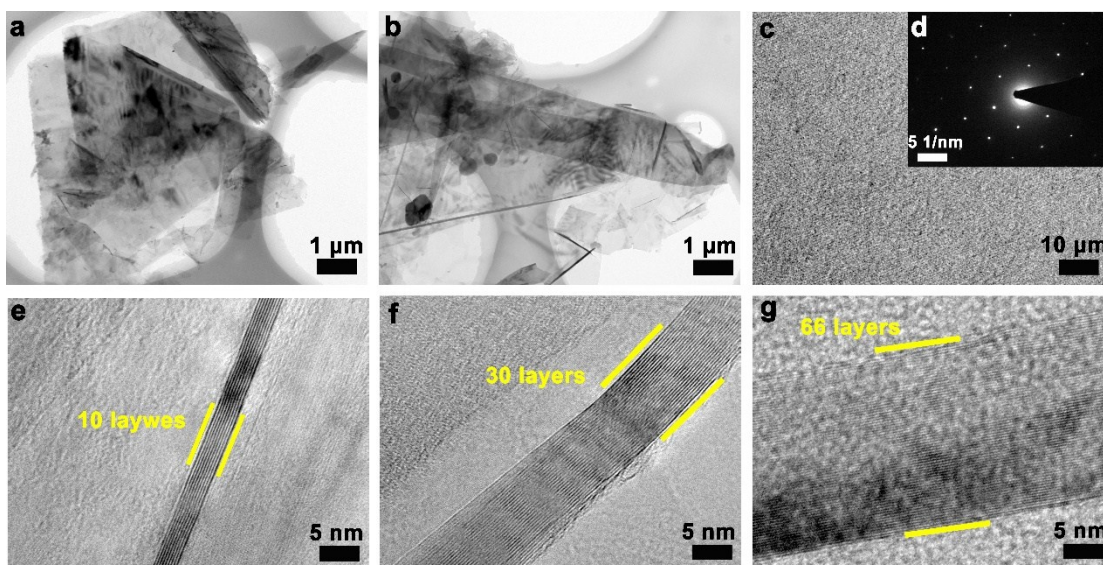


**Fig. S3.** TEM image of raw graphite foil used as anode (a-b). SAED diffraction pattern of graphite foil (c). HR-TEM image showing layer numbers of graphite foil (e-f).

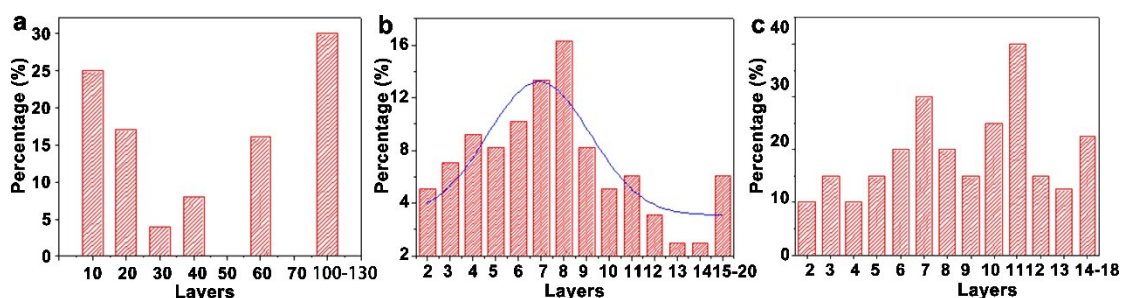


**Fig. S4.** (a) Thickness distribution histograms of layers of graphite foil (among 37 sheets) obtained by bath sonication in alcohol; (b-c) Thickness distribution histograms of peeled products using graphite foil (among 50 sheets) and HOPG (among 50 sheets) as anode after the electrochemical exfoliation (without bath sonication treatment), respectively.

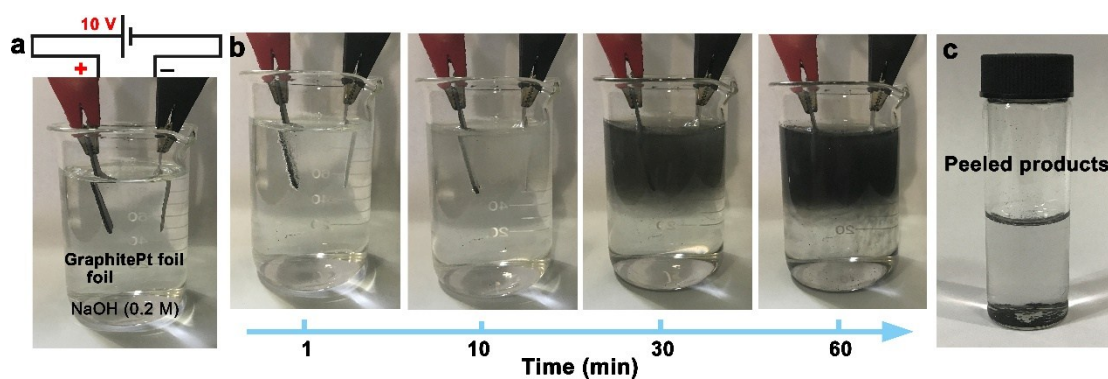


**Fig. S5.** Electrochemical exfoliation process using 0.2 M NaOH as electrolyte. (a) Schematic diagram of the electrochemical setup. (b-e) Digital photographs of electrochemical exfoliation in 60 minutes. (f) The peeled products were hardly dispersed in water.

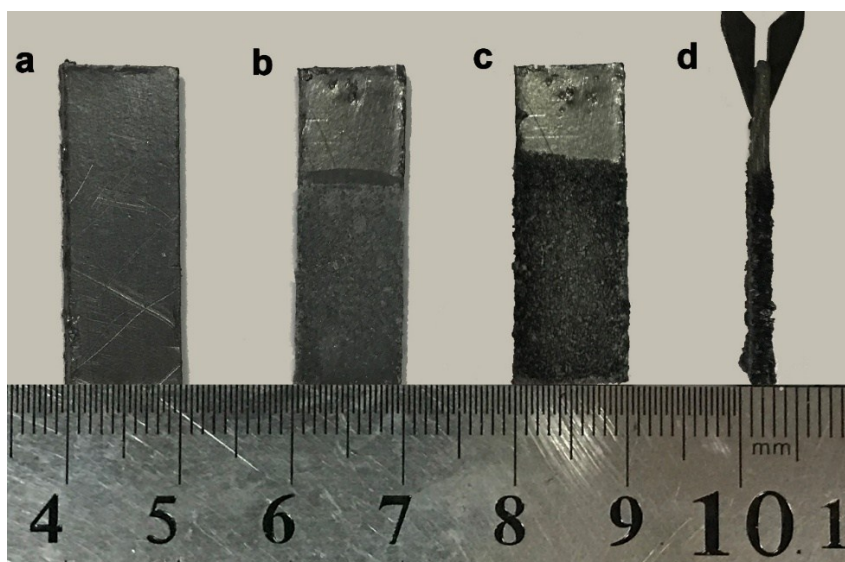


**Fig. S6.** The surface of graphite foil before (a) and after (b) the electrochemical process; The surface (c) and (d) side of graphite foil when exchanged to cathode.

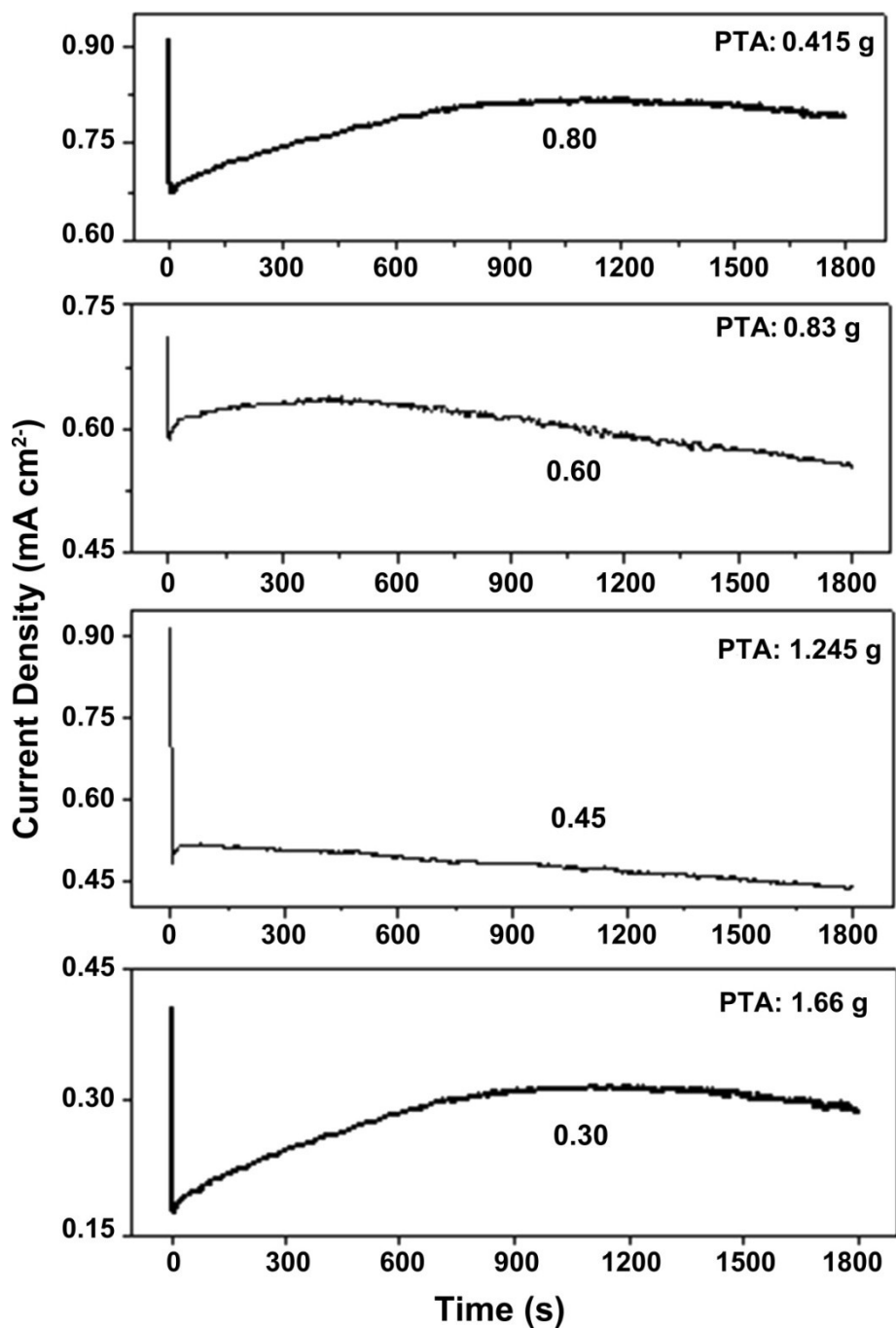


**Fig. S7.** Current density-time curves in different electrolytes of PTA and NaOH mixtures under 10V and 2 cm<sup>2</sup> graphite foil anode. Current densities at 1000 s anodization are 0.8, 0.6, 0.45 and 0.30 mA cm<sup>-2</sup> with PTA additions of 0.415g, 0.83g, 1.245g and 1.66g, respectively, in 100 mL DI water mixed with 0.8g NaOH. Besides, we have done the contrast experiment using NaOH (0.8 g, 100 mL DI water) as the electrolyte, and the current density gradually increased to 1.50 mA cm<sup>-2</sup> after 1000 s anodization.

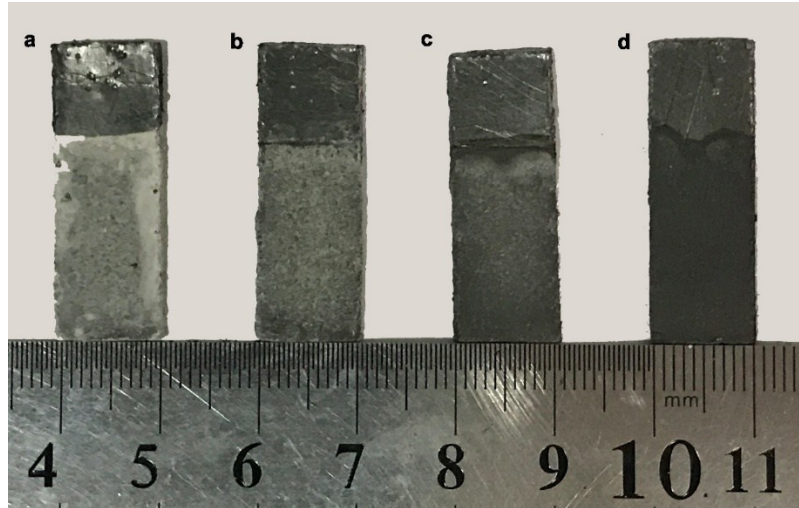


**Fig. S8.** The surface of graphite foil in above electrolytes (PTA contents were different from left to right: 0.415g, 0.83g, 1.245g and 1.66g, respectively) after the electrochemical process.

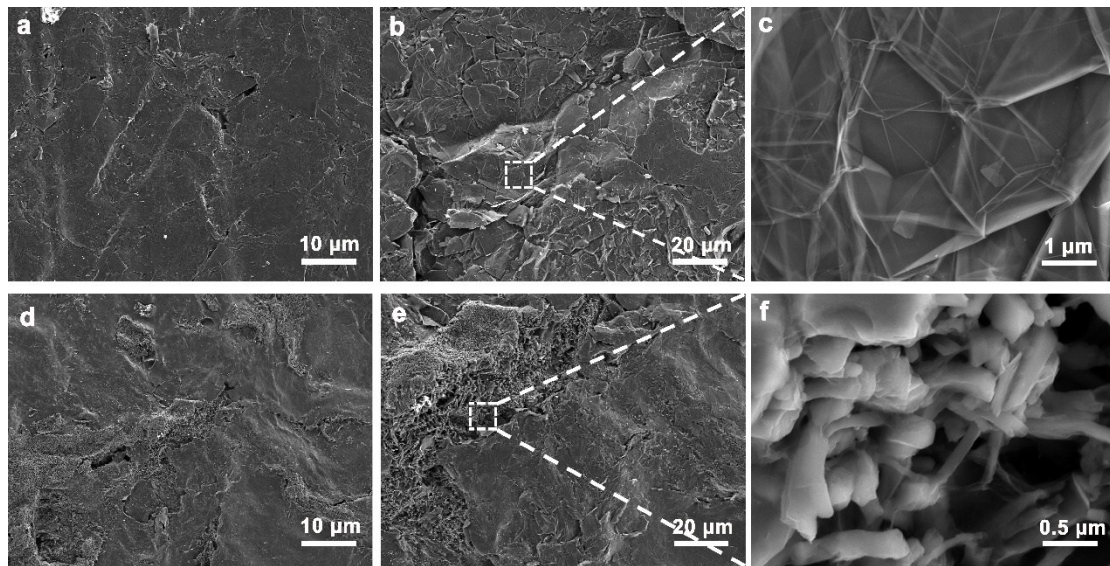


**Fig. S9.** SEM images of the surface of graphite foil (a-c) before and (d-f) after the electrochemical exfoliated process.

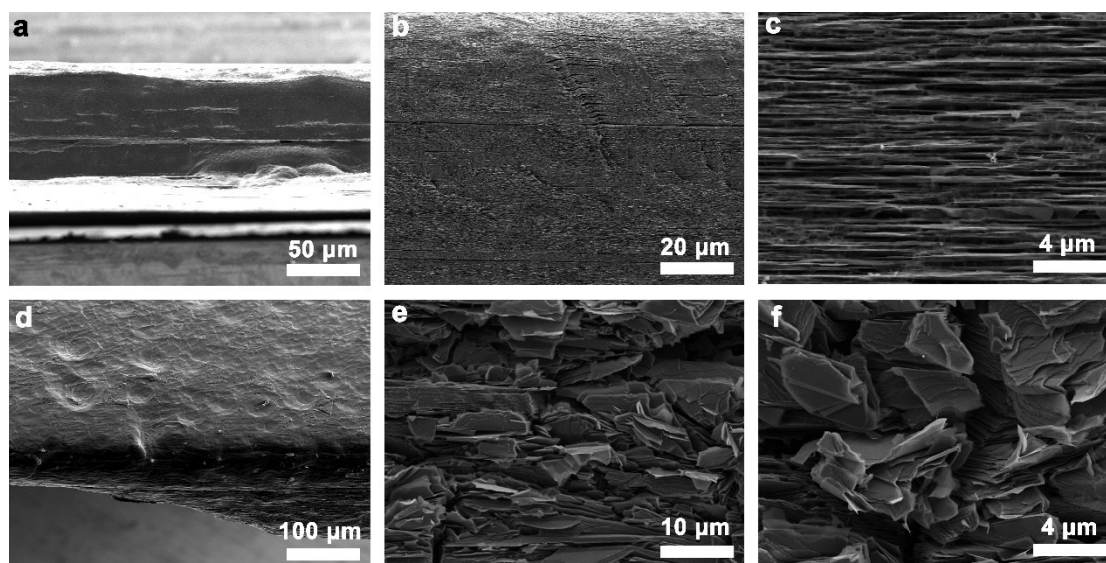


**Fig. S10.** SEM images of edge of HOPG used as anode. (a-c) the edge of HOPG before and (d-f) after the electrochemical exfoliated process.

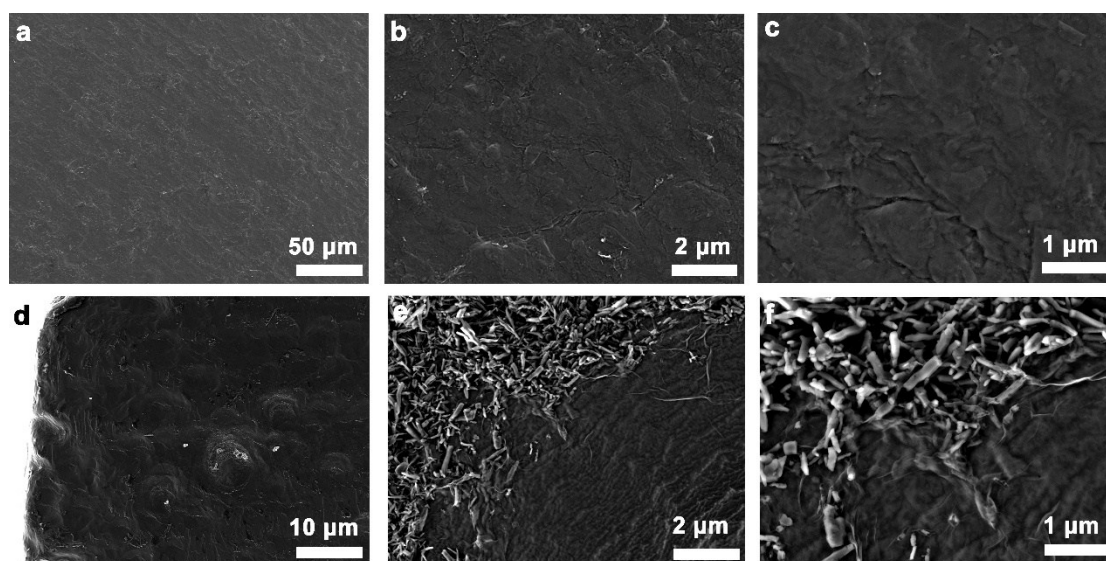


**Fig. S11.** SEM images of surface of HOPG used as anode. (a-c) the surface of HOPG before and (e-f) after the electrochemical exfoliated process.

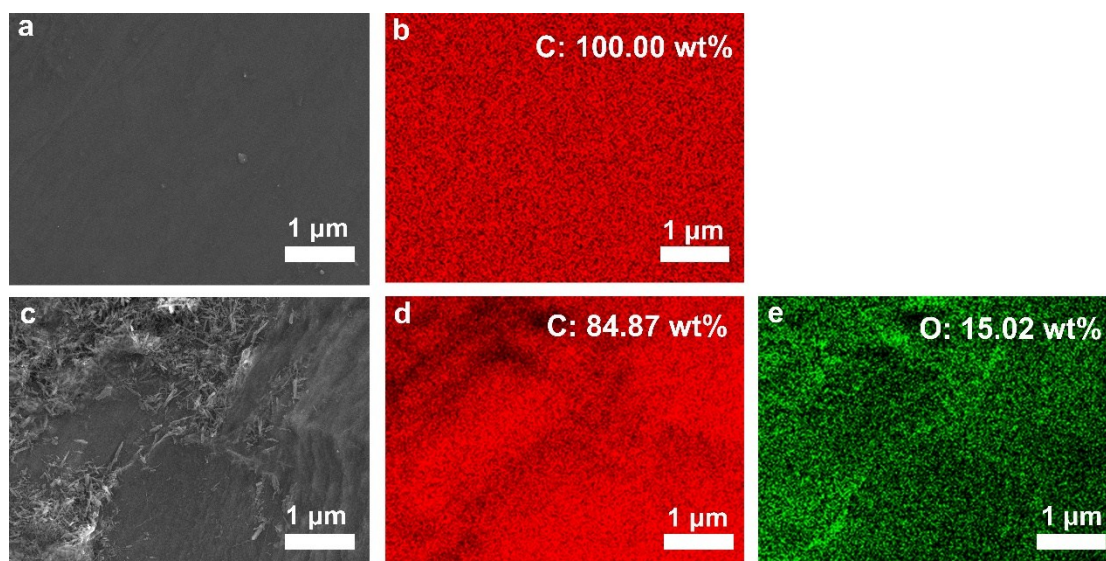


**Fig. S12.** (a) SEM image of HOPG before the electrochemical process. (b) C EDS mapping images of the surface of HOPG. (c) SEM image of HOPG after the electrochemical process. (d) C and (e) O EDS mapping images of HOPG after anodization.

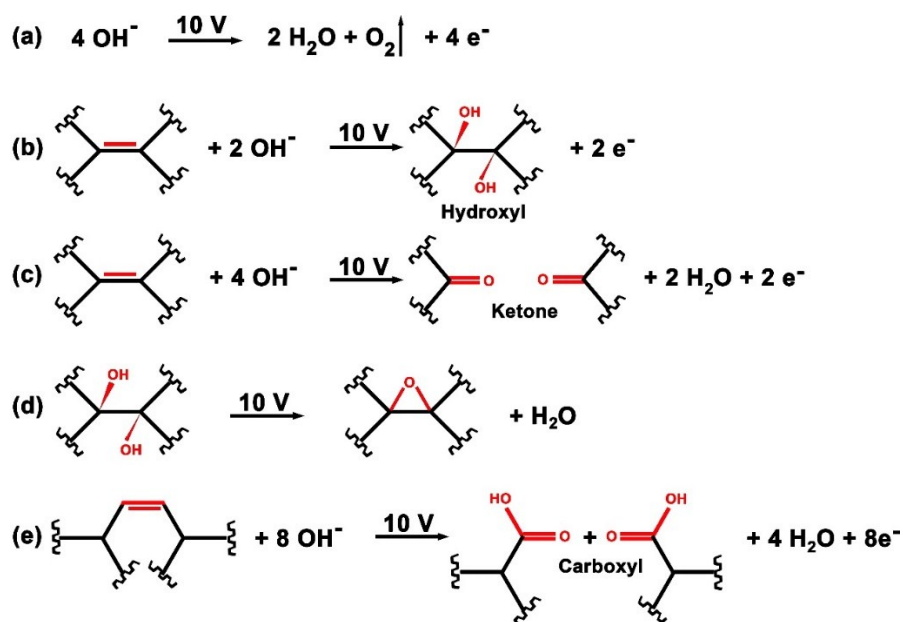


**Fig. S13.** The electrochemical reactions at graphite anode. The grafting of oxygen functional groups on graphene sheets is caused by the attack of oxygen-containing radicals.



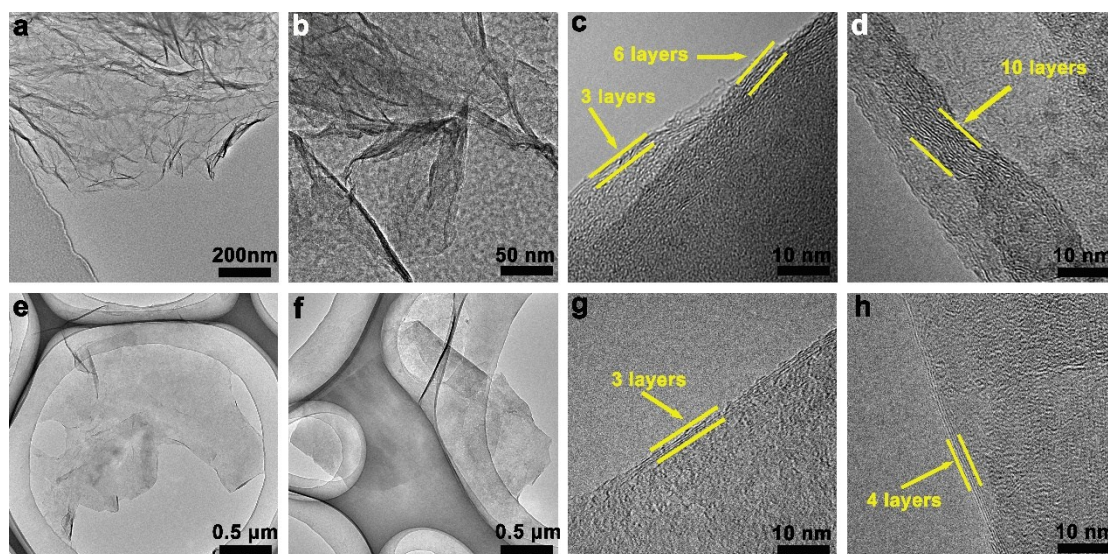


**Fig. S14.** Typical TEM and HRTEM images of the obtained graphene sheets. (a-d) the exfoliated graphene sheets without ultrasonic treatment; (e-h) the obtained graphene with 1h ultrasonic treatment in the electrolyte.

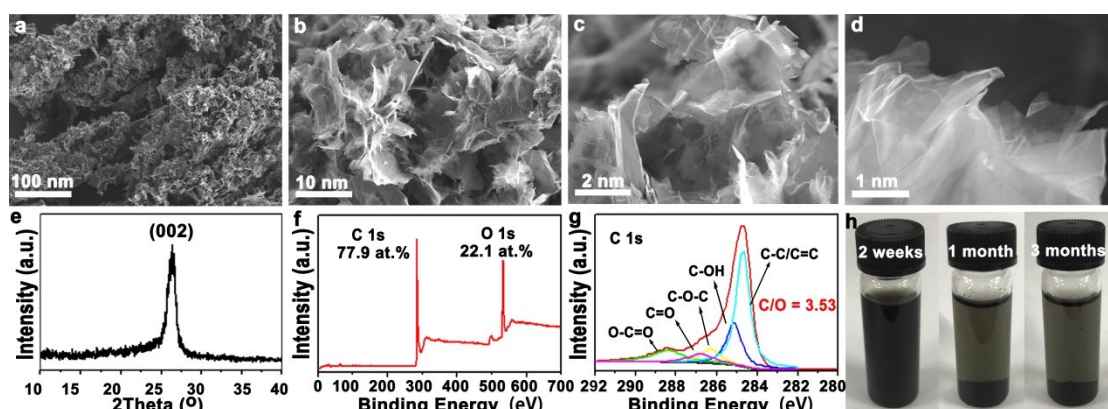


**Fig. S15.** Characterization of the product post electrochemical synthesis without any sonication treatment (3000 rpm,  $998\times g$ , centrifugal supernatant). (a-d) The SEM images of W-Gr powder. (e) XRD pattern. (f) XPS survey spectra, (g) XPS C 1s core-level spectrum. (h) The dispersion stability of the non-sonication product.

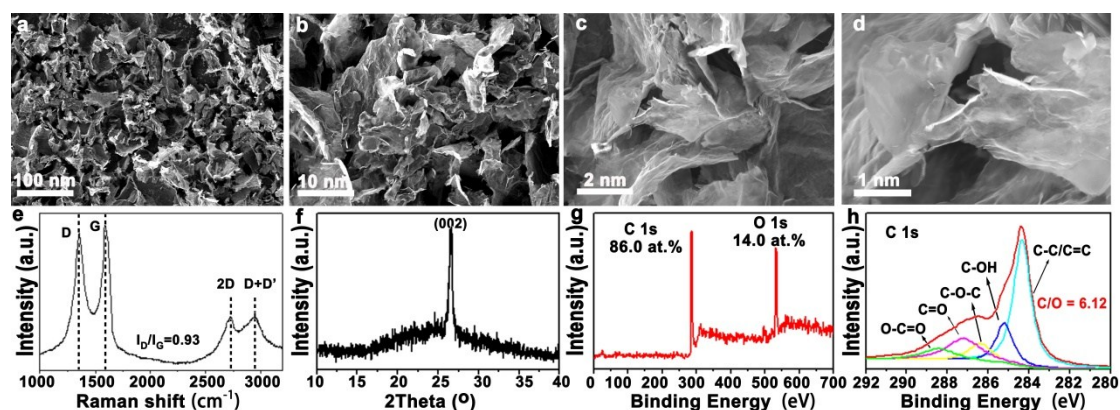
The SEM images (Fig. S15.a-d) show the glomerate morphology of product, indicating the poor dispersibility in aqueous solution without sonication assistant. This can be attributed to the thicker graphene sheets prepared by electrochemical exfoliation.<sup>1,2</sup>

Fig. S15e shows the XRD patterns of the product. A broad diffraction hump ranging in  $20\text{--}30^\circ$  of the XRD pattern indicates the exfoliation of graphene sheets during the

electrochemical process and the lack of the long-range order due to the oxygen-functionalities. A weak peak centered at  $25.2^\circ$  is attributed to the characteristic of graphite flakes that not fully exfoliated by electrochemical exfoliation.

The XPS measurements were performed to assess the oxygen content before (oxygen content: 22.1 at%) and after 1 h sonication (oxygen content: 22.6 at%). The similar results indicated the adequate oxidation during the electrochemical process. The higher oxygen content of the final W-Gr product was attributed to the hydroxylation reaction during the sonication process. More oxygen functional groups can be grafted on the electrochemical exfoliated products during the 1 h sonication treatment.<sup>1</sup>

Moreover, the attempts (such as vibration and agitation) to disperse the product post the electrochemical process were ineffectual. The aqueous dispersions of the electrochemical exfoliated products with different months were shown in Fig. S15h, which proved the poor dispersibility without sonication treatment.



**Fig. S16.** Characterization of the non-sonication product post electrochemical synthesis (3000 rpm,  $998\times g$ , centrifugal precipitate). (a-d) The SEM images. (e) Raman spectra. (f) XRD pattern. (g) XPS survey spectra, (h) XPS C 1s core-level spectrum.

The yield of W-Gr is higher than 87.3% ( $\sim 10\%$  graphite flakes left), while the yield of W-Gr post electrochemical exfoliation without sonication is 25-35%, which demonstrate the essential role of sonication. The detail analysis of the sample was shown in Fig. S16.

The low-magnification SEM images of the freeze-drying power sample (non-sonication precipitate) were shown in Fig. S16a-c, indicated the crumpled and

superimposed morphology in aqueous solution. The high-magnification SEM image (Fig. S16d) shows a flexible morphology, confirming the transformation of graphene sheets from graphite anode was happened during the electrochemical process.

The Raman spectrum of the sample was shown in Fig. S16e. The strong D and D' peak appeared in the spectrum (Fig. S16e), which were activated by a single-phonon intravalley scattering process,<sup>3</sup> indicating the presence of abundant defects and domain boundaries.<sup>4</sup> It has been well acknowledged that the intensity ratio of the D peak to the G peak ( $I_D/I_G \sim 0.93$ ) is attributed to the content of defects, such as the gifting of oxygen functional groups and some damages of structure.

The XRD patterns of non-sonication precipitation were shown in Fig. S16f. A broad diffraction hump ranging in  $17\text{--}30^\circ$  of the XRD pattern also indicates the exfoliation of graphene sheets and the lack of the long-range order of due to oxygen-functionalities. A weak peak centered at  $25.2^\circ$  was attributed incompletely exfoliation of the graphite flacks.

The XPS measurements (Fig. S16g, h) were performed to assess the oxygen content (14.9 at.%) of the non-sonication precipitation. The lower oxygen content (compared to the W-Gr products) indicated the inadequate oxidation of the peeled products during the electrochemical process. This result reconfirmed that the products were composed of the exfoliated graphene sheets (adequate oxidation) and the peeled graphitized flakes (inadequate oxidation).

Thus, the sonication treatment can assist the dispersion of exfoliated graphene sheets in aqueous solution. Meanwhile, it is also crucial for the further exfoliation of the flakes those adequately oxidized but incomplete exfoliated by electrochemical delamination to further increase the yield of few-layer graphene sheets.<sup>2</sup>

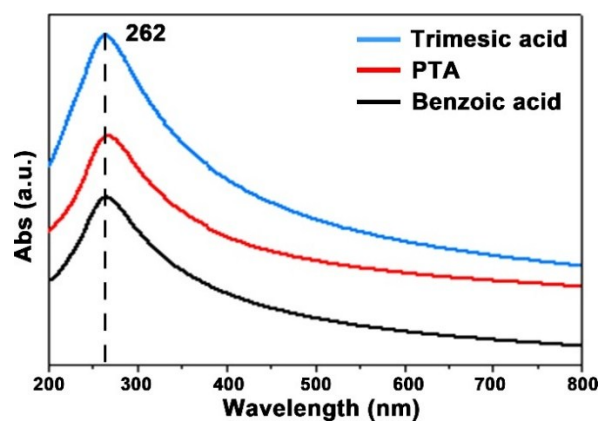


**Fig. S15.** UV-Vis spectra of W-Gr aqueous dispersions using trimesic acid (blue line), PTA (red line) and benzoic acid (black line) dissolved in alkaline aqueous solution as electrolyte, respectively.

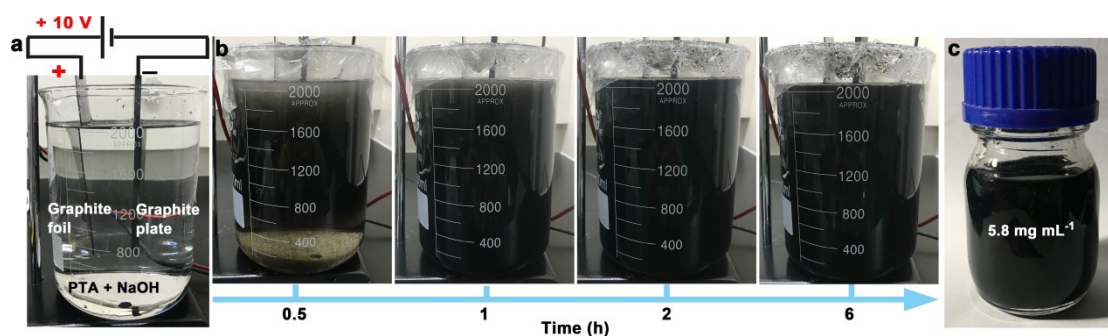


**Fig. S17.** The large-scale electrochemical exfoliation of W-Gr. (a) Schematic diagram of the preparing setup. (b) Digital photographs showing the evolution of the electrochemical process. (c) The obtained large-scale W-Gr dispersion.

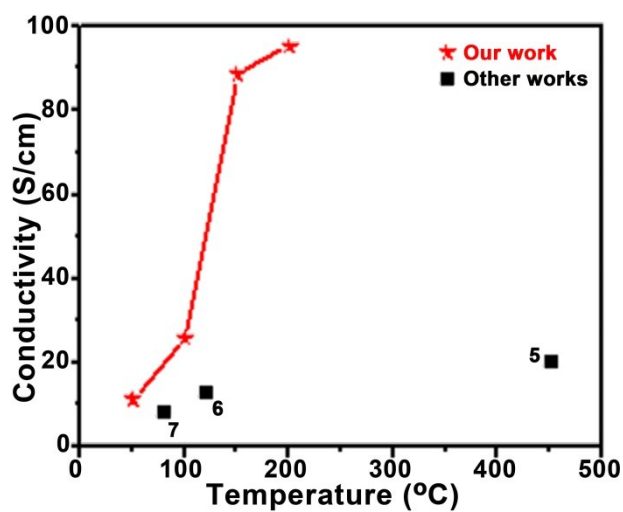


**Fig. S18.** The conductivity of W-Gr films after heat treatment at different temperatures in this work and in other reported works.

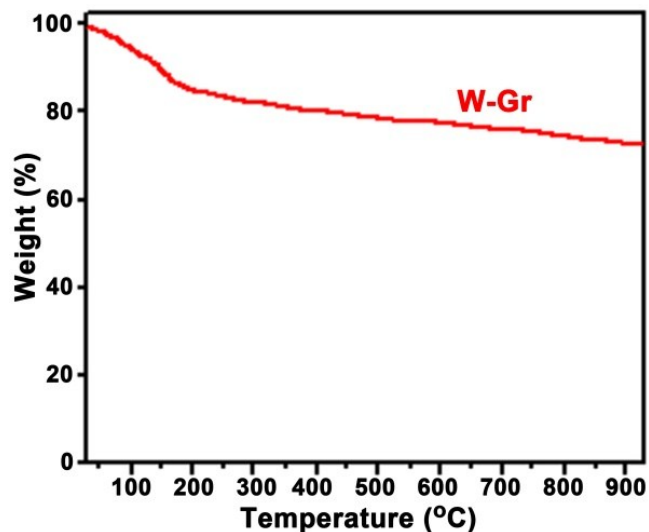


**Fig. S19.** TGA curves of the exfoliated W-Gr sheets in nitrogen atmosphere (N<sub>2</sub>).

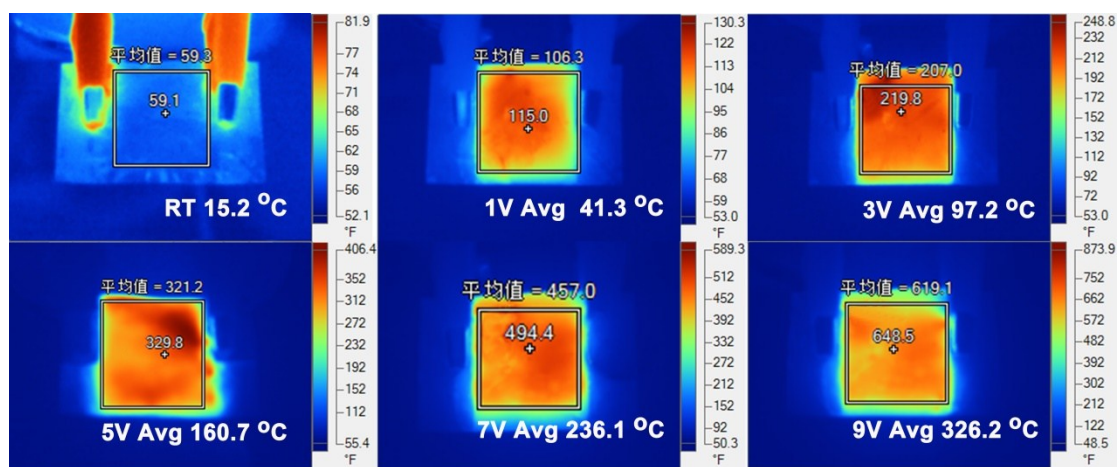


**Fig. S20.** Infrared thermal images showing the equilibrium temperatures (15.2, 41.3, 97.2, 160.7, 236.1 and 326.2 °C) of W-Gr electrothermal film under various heating voltages: (a) 0, 1, 3, 5, 7 and 9 V.

**Video 1.** The phenomenon of the electrodes (anode: graphite foil, cathode: platinum foil) when the potential (+ 10V) applied and the phenomenon of the electrodes when transfer the potential into -10 V.

**Video 2.** The phenomenon of the electrodes (both platinum foils) when the potential (+ 10V) applied and the phenomenon of the electrodes when transfer the potential into -10 V.

**Table S1.** Comparison of experimental conditions and results

Entry	Electrolyte	Voltage (V)	C/O	Concentration (g/L)	Results
1	NaOH (0.8 g), 100 ml DI water	10	/	/	Contrast experiment. The exfoliated graphite particles were barely dispersed in water.
2	PTA (8 g), NaOH (8.3 g), 200 ml DI water	10		0.5	The exfoliated process is fast and the obtained graphene sheets are easily aggregated in a few days.
3	PTA (0.83 g), NaOH (0.8 g), 100 ml DI water	6.5	/	0.9	/
4		8.5	4.45	1.1	The obtained graphene can hardly disperse in water. The product yield is less than 30%.
5		10	4.02	8.2	The graphene can stably disperse in water with high concentration. The product yield is 87.3 %.
6		15	4.38	3.9	The exfoliated process is faster. The product yield is less than 50 %.
7		20	4.53	2.0	The product yield is 32 %.
8	Benzoic acid (0.61 g), NaOH (0.4 g), 100 ml H <sub>2</sub> O	12	4.42	3.2	The obtained graphene sheets can disperse in water.
9	Trimesic acid (1.05 g), NaOH (1.2 g), 100 ml H <sub>2</sub> O	8	4.23	1.4	The reaction rate is fast. The obtained graphene sheets can disperse in water.

**Table S2.** Comparison of the maximum aqueous concentration of W-Gr and corresponding electrical conductivity after thermal reduction in different reports.

Method	Main reagents	Concentration (g/L)	Conductivity (S/m)	Temperature (°C)	Ref.
Electrochemical method	<b>PTA/NaOH</b>	<b>8.2</b>	<b>8865</b>	<b>150 (for 1h)</b>	<b>This work</b>
Chemical	H <sub>2</sub> O <sub>2</sub>	10.3	2 000	450	5

modification				(for 120 s)	
	Sulfanilic acid, N <sub>2</sub> H <sub>4</sub>	2.0	1 250	120	6
	L-ascorbic acid	0.1	800	80 (for 12h)	7

### Ref.

1. C. Cheng, D. Li, *Adv. Mater.*, 2013, **25(1)**, 13-30.
2. J. Sun, Y. Deng, J. Li, G. Wang, P. He, S. Tian, X. M. Bu, Z. F. Di, S. W. Yang, G. Q. Ding and X. M. Xie, *ACS Appl. Mater. Interfaces.*, 2016, **8(16)**, 10226-10233.
3. F. Tuinstra, J. L. Koenig, *J. Chem. Phys.*, 1970, **53**, 1126.
4. P. Venezuela, M. Lazzeri, F. Mauri, *Phys. Rev. B*, 2011, **84**, 035433.
5. X. F. You, S. W. Yang, J. P. Li, Y. Deng, L. Q. Dai, X. Peng, H. G. Huang, J. Sun, G. Wang, P. He, G. Q. Ding and X. M. Xie, *ACS Appl. Mater. Interfaces.*, 2017, **9(3)**, 2856-2866.
6. Y. Si, E. T. Samulski, *Nano lett.*, 2008, **8**, 1679-1682.
7. J. Zhang, H. Yang, G. Shen, P. Cheng, J. Zhang and S. Guo, *Chem. Commun*, 2010, **46**, 1112-1114.